Proceedings of the International Conference on Oxide Materials for Electronic Engineering, May 29–June 2, 2017, Lviv

Synthesis and Structure Characterisation of Micro-and Nanocrystalline Powders of $Dy_{1-x}R_xFeO_3$ (R = La, Pr, Nd, Sm, Gd)

O. Pavlovska[a,*], I. Lutsyuk[b], A. Kondyr[c], Ya. Zhydachevskyy[a,d], Ya. Vakhula[b], A. Pieniążek[d] and L. Vasylechko[a]

[a]Semiconductor Electronics Department of Lviv Polytechnic National University, 12 Bandera Str., 79013 Lviv, Ukraine

[b]Department of Chemical Technology of Silicates of Lviv Polytechnic National University, 12 Bandera Str., 79013 Lviv, Ukraine

[c]Department of Applied Physics and Nanomaterials Science of Lviv Polytechnic National University, 12 Bandera Str., 79013 Lviv, Ukraine

[d]Institute of Physics, Polish Academy of Sciences, Aleja Lotnikow 32/46, PL-02668 Warsaw, Poland

This work deals with the study of the phase and crystal structure behaviour of new micro- and nanocrystalline ferrites $Dy_{1-x}R_xFeO_3$ obtained by solid state reactions (R = La, Pr) and sol–gel citrate (R = Nd, Sm, Gd) techniques. It was established that all synthesized samples adopt orthorhombic perovskite structure isotypic with $GdFeO_3$. Unit cell dimensions and atomic coordinates of the mixed rare earth ferrites derived by full profile Rietveld refinement technique agree well with the data of the "pure" $DyFeO_3$ and $RFeO_3$ compounds, thus proving formation of continuous solid solutions $Dy_{1-x}R_xFeO_3$ in the $DyFeO_3$–$RFeO_3$ systems (R = La, Pr, Nd, Sm, Gd). Peculiarity of the $Dy_{1-x}La_xFeO_3$ series is the lattice parameters crossover and formation of dimensionally tetragonal structure at $x \approx 0.97$.

DOI: 10.12693/APhysPolA.133.802

PACS/topics: 61.66.Fn, 61.05.cp

1. Introduction

Complex oxides with perovskite structure $RFeO_3$, where R are rare earth elements, represent an important class of functional materials. $RFeO_3$ compounds are used in thermoelectric devices, solid oxide fuel cells [1], as membranes for gases separation, sensory materials and catalysts [2–4], as magnetic and multiferroics materials [5, 6]. Complementary, the interest to the rare earth ferrites is stimulated by their specific fundamental physical properties and interesting high temperature magnetic behaviour, namely, spin-reorientation phenomena and the para- to antiferomagnetic transition which occur in $RFeO_3$ series at 620–750 K [7–9]. Just recently interesting phenomena of magnetoelastic coupling were detected in $SmFeO_3$ and some solid solutions based on them [10, 11]. Recently, versatile and gigantic magnetoelectric phenomena have been found for a single crystal of $DyFeO_3$ [12]. It was revealed that application of magnetic field along the c axis induces a multiferroic phase with magnetization and electric polarization both along the c axis. In this respect, several mixed $DyFeO_3$-based systems, such as $Dy_{1-x}La_xFeO_3$ [13], $Dy_{1-x}Pr_xFeO_3$ [14, 15], $Dy_{1-x}Ho_xFeO_3$ [16], $Dy_{1-x}Er_xFeO_3$ [17] and $Dy_{1-x}Tm_xFeO_3$ [18] were studied in the last decade. However, no structural parameters were reported for the majority of $Dy_{1-x}R_xFeO_3$ systems. The aim of the present work is a study of crystal structure behaviour of new micro- and nanocrystalline ferrites $Dy_{1-x}R_xFeO_3$ (R = La, Pr Nd, Sm, Gd) obtained by solid state and sol–gel citrate techniques.

2. Experimental

New mixed orthoferrites $Dy_{1-x}R_xFeO_3$ (R = La, Pr, Nd, Sm, Gd) were obtained by two different methods. The samples containing La and Pr were synthesized by solid state reactions technique according to the following reaction schemes:

$$(1-x)Dy_2O_3 + xLa_2O_3 + Fe_2O_3 \rightarrow 2Dy_{1-x}La_xFeO_3,$$

$$3(1-x)Dy_2O_3 + xPr_6O_{11} + 3Fe_2O_3 \rightarrow 6Dy_{1-x}Pr_xFeO_3 + xO_2 \uparrow .$$

Stoichiometric amounts of precursor oxides La_2O_3, Pr_6O_{11}, Dy_2O_3 and Fe_2O_3 were ball-milled in ethanol for 4 h, dried, and heat treated in alundum crucibles in air at 1473 K for 80 h. As obtained products were repeatedly heat treated in air subsequently at 1673 K for 25 h and at 1773 K for 25 h, after that slowly cooled to the room temperature (RT). For preparation of nanocrystalline powders of $Dy_{0.5}R_{0.5}FeO_3$ (R = Nd, Sm, Gd) a low-temperature sol–gel citrate method was used. Rare earth oxides Dy_2O_3, Sm_2O_3 and Gd_2O_3 as well as $Nd(NO_3)_2 \cdot 6H_2O$ and $Fe(NO_3)_2 \cdot 9H_2O$ were used as an initial reagents. Neodymium and iron nitrates were dissolved in distilled water, whereas nitrate solutions of Dy,

*corresponding author; e-mail: olena_kuz@i.ua

Sm, and Gd were prepared by dissolving of corresponding oxides in HNO_3. Appropriate amounts of corresponding solutions were mixed on magnetic stirring for 30 min, after that water solution of citric acid (CA) and ethyleneglycol (EG) were sequentially added to the reaction mixture under continuous stirring. The molar ratio of reagents was $n(Dy^{3+}):n(R^{3+}):n(Fe^{3+}):n(CC):n(EG) = 0.5 : 0.5 : 1 : 2 : 1$ (R = Nd, Sm, Gd). As prepared solutions were gelled at 373–393 K for 4 h after that heat treated sequentially at 573 K and 723 K for 1 h. The foamy product obtained was finally calcined at 1273 K for 2 h. In such a way single phase nanocrystalline powders of $Dy_{0.5}R_{0.5}FeO_3$ were obtained with average grain size of 86–300 nm.

X-ray powder diffraction technique (Huber imaging plate Guinier camera G670, Cu $K_{\alpha 1}$ radiation, $\lambda = 1.54056$ Å) was used for the phase and structural characterization of the samples at room temperature. Structural parameters, average crystallite size of the powders (D, [nm]) and microstresses ($\langle\varepsilon\rangle = \langle\Delta d\rangle/d$, [%]) of the samples were derived from the experimental diffractograms by using full profile Rietveld refinement technique applying WinCSD program package [19]. The morphology of sol–gel derived $Dy_{0.5}R_{0.5}FeO_3$ (R = Nd, Sm, Gd) series was investigated by means of Hitachi SU-70 scanning electron microscope.

3. Results and discussion

X-ray powder diffraction examination revealed that $Dy_{1-x}R_xFeO_3$ (R = La, Pr) samples synthesized by solid state method adopt orthorhombic perovskite structure isotypic with $GdFeO_3$. No traces of foreign phases were detected. Refinement of crystal structures in space group *Pbnm* by using full profile Rietveld method shows excellent agreement between the experimental X-ray powder diffraction pattern (red dots) and calculated pattern (blue line) (Fig. 1) thus proving a phase purity and crystal structure of the samples.

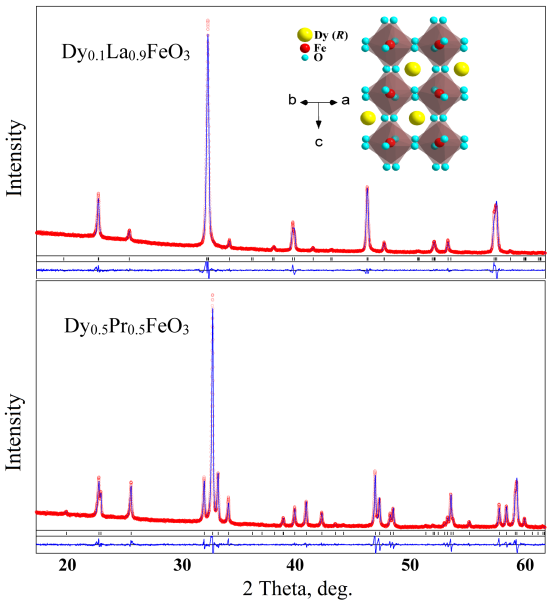

Fig. 1. Graphical results of the Rietveld refinement of the $Dy_{0.1}La_{0.9}FeO_3$ and $Dy_{0.5}Pr_{0.5}FeO_3$ structures. The difference between measured (red) and calculated (blue) XRD profiles is shown as a curve below the diagrams. Short vertical bars indicate the positions of diffraction maxima in *Pbnm* structure. Inset shows polyhedral representation of orthorhombic $Dy_{1-x}R_xFeO_3$ structure.

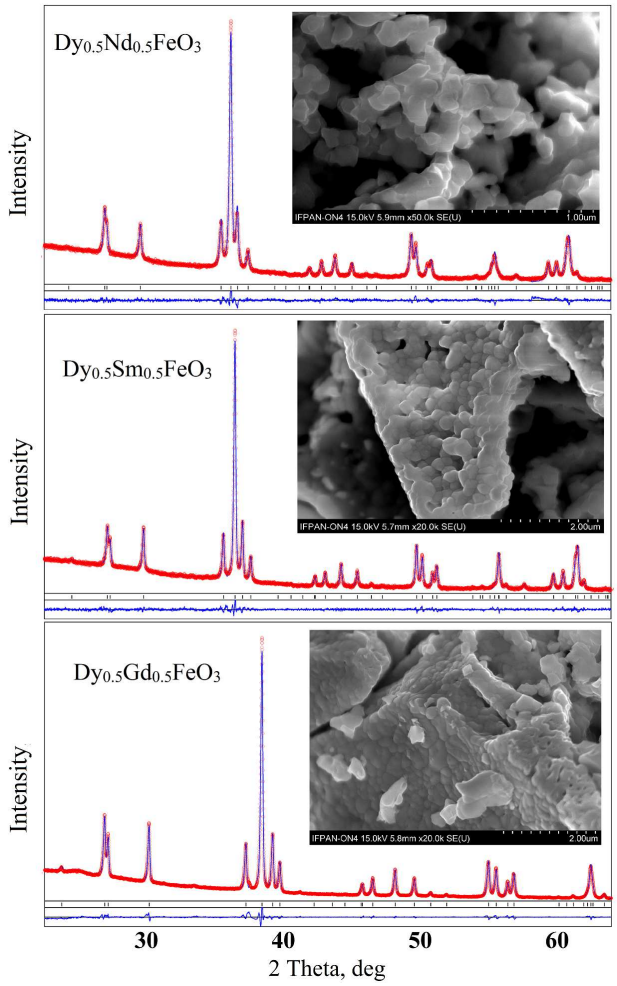

Fig. 2. Graphical results of the Rietveld refinement of $Dy_{0.5}Nd_{0.5}FeO_3$, $Dy_{0.5}Sm_{0.5}FeO_3$ and $Dy_{0.5}Gd_{0.5}FeO_3$ structures, obtained by sol–gel citrate method and SEM pictures of these materials (insets).

Examination of X-ray diffraction patterns of sol–gel derived $Dy_{0.5}R_{0.5}FeO_3$ (R = Nd, Sm, Gd) materials revealed that even short-term heat treatment at 1273 K for 2 h led to formation of pure perovskite structure. Graphical results of the Rietveld refinement of as-obtained $Dy_{0.5}R_{0.5}FeO_3$ materials are presented in Fig. 2. Detectable peak broadening in the XRD patterns indicate nanoscale grains size of sol–gel derived specimens. Indeed, evaluation of microstructural parameters of the $Dy_{0.5}Nd_{0.5}FeO_3$, $Dy_{0.5}Sm_{0.5}FeO_3$, and $Dy_{0.5}Gd_{0.5}FeO_3$ samples from the analysis of the XRD profile broadening by full profile Rietveld technique, lead to the average grain size $D_{ave} = 86$, 121, 316 nm and microstrains

$\langle\varepsilon\rangle = \langle\Delta d\rangle/d = 0.15\%$, 0.07% and 0.09%, respectively. Scanning electron microscopy of $Dy_{0.5}R_{0.5}FeO_3$ (R = Nd, Sm, Gd) samples (Fig. 2, insets) revealed a lacy morphology of the powders consisting of irregular shaped nanoparticles.

Refined structural parameters of all micro- and nanocrystalline $Dy_{1-x}R_xFeO_3$ samples synthesized, as well as corresponding residuals are presented in Table I.

TABLE I

Lattice parameters, coordinates and displacement parameters of atoms in $Dy_{1-x}R_xFeO_3$ (R = La, Pr, Nd, Sm, Gd) structures.

Atoms sites	Parameters residuals	$Dy_{0.7}La_{0.3}FeO_3$	$Dy_{0.1}La_{0.9}FeO_3$	$Dy_{0.5}Pr_{0.5}FeO_3$	$Dy_{0.5}Nd_{0.5}FeO_3$	$Dy_{0.5}Sm_{0.5}FeO_3$	$Dy_{0.5}Gd_{0.5}FeO_3$
	a [Å]	5.3723(2)	5.5323(4)	5.3955(3)	5.3805(2)	5.3490(1)	5.3258(5)
	b [Å]	5.5929(3)	5.5635(4)	5.5921(3)	5.5874(2)	5.5904(1)	5.5984(6)
	c [Å]	7.6925(4)	7.8324(6)	7.7082(4)	7.6944(3)	7.6612(2)	7.6439(7)
	V [Å^3]	231.13(4)	241.07(6)	232.57(4)	231.31(3)	229.09(2)	227.91(7)
Dy(R), 4c	x	-0.0152(2)	-0.0108(2)	-0.0124(2)	-0.0104(4)	-0.0154(2)	-0.0167(9)
	y	0.0623(2)	0.0337(1)	0.0576(2)	0.0565(2)	0.0609(1)	0.0642(6)
	z	$\frac{1}{4}$	$\frac{1}{4}$	$\frac{1}{4}$	$\frac{1}{4}$	$\frac{1}{4}$	$\frac{1}{4}$
	B_{iso} [Å^2]	0.46(2)	0.44(2)	0.63(2)	0.81(2)	1.21(2)	1.18(2)
Fe, 4b	x	0	0	0	0	0	0
	y	$\frac{1}{2}$	$\frac{1}{2}$	$\frac{1}{2}$	$\frac{1}{2}$	$\frac{1}{2}$	$\frac{1}{2}$
	z	0	0	0	0	0	0
	B_{iso} [Å^2]	1.27(5)	1.50(4)	0.95(5)	1.03(5)	1.32(4)	1.14(4)
O1, 4c	x	0.0965(15)	0.035(3)	0.0886(14)	0.104(2)	0.1017(13)	0.1082(6)
	y	0.442(2)	0.472(2)	0.4624(13)	0.438(2)	0.4570(13)	0.4612(6)
	z	$\frac{1}{4}$	$\frac{1}{4}$	$\frac{1}{4}$	$\frac{1}{4}$	$\frac{1}{4}$	$\frac{1}{4}$
	B_{iso} [Å^2]	2.5(2)	2.3(4)	1.9(3)	1.7(3)	2.1(3)	0.77(13)
O2, 8d	x	-0.3326(10)	-0.314(2)	-0.2830(11)	-0.3155(12)	-0.3022(10)	-0.3025(5)
	y	0.3093(11)	0.284(2)	0.2741(11)	0.2958(13)	0.2933(11)	0.3034(5)
	z	0.0539(7)	0.0240(13)	0.0637(6)	0.0531(9)	0.0527(7)	0.0542(3)
	B_{iso} [Å^2]	0.8(2)	1.6(3)	0.8(2)	0.5(2)	1.8(2)	1.53(10)
	R_I	0.070	0.048	0.060	0.091	0.077	0.042
	R_P	0.169	0.159	0.187	0.188	0.133	0.074

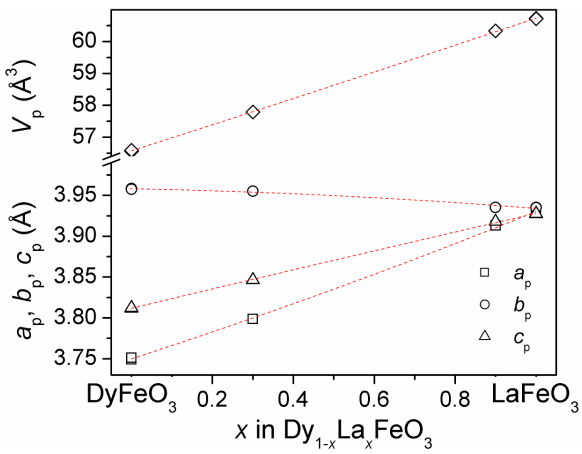

Fig. 3. Concentration dependences of unit cell dimensions of $Dy_{1-x}La_xFeO_3$. Orthorhombic lattice parameters and unit cell volume are normalized to the perovskite ones as follows: $a_p = a_0/\sqrt{2}$, $b_p = b_0/\sqrt{2}$, $c_p = c_0/2$, $V_p = V_0/4$. The dashed lines are polynomial fits: $a_p(x) = 3.750 + 0.16x + 0.02x^2$; $b_p = 3.958 - 0.01x - 0.015x^2$; $c_p = 3.8118 + 0.119x - 0.002x^2$; $V_p = 56.58 + 4.5x + 0.1x^2$.

Structural parameters of the mixed $Dy_{1-x}R_xFeO_3$ ferrites obtained agree well with the data for the "pure" $RFeO_3$ compounds, thus proving formation of continuous solid solutions with orthorhombic perovskite structure in the $DyFeO_3$–$RFeO_3$ (R = La, Pr, Nd, Sm, Gd) systems. Peculiarity of the $Dy_{1-x}La_xFeO_3$ series is the lattice parameters crossover and formation of dimensionally tetragonal structures at $x \approx 0.97$ (Fig. 3). Such strongly anisotropic behaviour of the unit cell dimensions, which was also recently observed in the related in $La_{1-x}Sm_xFeO_3$ series [20], is explained by crystal structure peculiarities of the end members of the systems. In spite of being isostructural, $DyFeO_3$ and $LaFeO_3$ show different order of the perovskite cell parameters: $b_p > c_p > a_p$ and $b_p > a_p > c_p$, respectively. As a result, a crossover of a_p- and c_p-parameters occurs in $Dy_{1-x}R_xFeO_3$ system. Similar phenomena were earlier observed in the related cobaltite-ferrites $RCo_{1-x}Fe_xO_3$ [21, 22], as well as among isostructural rare earth perovskites $R_{1-x}R'_xAl(Ga)O_3$ [23, 24], in which end members of the systems possess different relations of the unit cell dimensions.

Figure 4 demonstrates evolution of the lattice parameters and unit cell volumes in $Dy_{0.5}R_{0.5}FeO_3$ series versus ionic radii of rare earth cations. The perovskite lattice parameters show anisotropic convergent behaviour: the

a- and c-parameters increases with increasing R-cation radii, whereas b-parameter decreases (Fig. 4). However, the unit cell volumes in $Dy_{1-x}R_xFeO_3$ series increases almost linearly according to the Vegard rule. This observation indicates statistical distribution of dysprosium and rare earth species over positions of A-cations in $Dy_{1-x}R_xFeO_3$ perovskite structures.

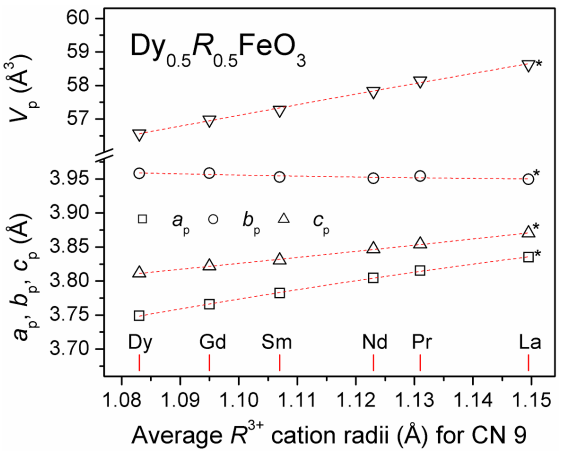

Fig. 4. Dependences of the unit cell parameters versus of average R-cation radii. The values indicated by asterisks are calculated from polynomial fits of the data presented in Fig. 3.

4. Conclusions

Series of micro- and nanocrystalline powders of $Dy_{1-x}R_xFeO_3$ were obtained by solid state reactions in air at 1773 K (R = La, Pr) and by a wet sol–gel citrate route at 1273 K (R = Nd, Sm, Gd). In comparison with a traditional energy-consuming high-temperature ceramic technique, the low-temperature sol–gel citrate method is very promising tool for a synthesis of the phase pure fine powders of mixed perovskite ferrites. Both micro- and nanocrystalline series of the samples synthesized adopt orthorhombically distorted perovskite structure isotypic with $GdFeO_3$. Obtained structural parameters of $Dy_{1-x}R_xFeO_3$ ferrites prove the formation of continuous solid solutions in $DyFeO_3$–$RFeO_3$ (R = La, Pr, Nd, Sm, Gd) pseudobinary systems. Peculiarity of $Dy_{1-x}La_xFeO_3$ solid solution is divergence behaviour of unit cells dimensions with increasing lanthanum content and crossover of the a and c perovskite lattice parameters at $x \approx 0.97$.

Acknowledgments

The work was supported in parts by the Ukrainian Ministry of Education and Sciences (Project "RZE" and "Feryt") and ICDD Grant-in-Aid program.

References

[1] Ch. Sun, R. Hui, J. Roller, *J. Solid State Electrochem.* **14**, 1125 (2009).

[2] M.R. Goldwasser, M.E. Rivas, M.L. Lugo, E. Pietri, J. Pérez-Zurita, M.L. Cubeiro, A. Griboval-Constant, G. Leclercq, *Catal. Today* **107-108**, 106 (2005).

[3] Y. Wang, X. Yang, L. Lu, X. Wang, *Thermochim. Acta* **443**, 225 (2006).

[4] J. Ding, X. Lü, H. Shu, J. Xie, H. Zhang, *Mater. Sci. Eng. B* **171**, 31 (2010).

[5] Y. Tokunaga, N. Furukawa, H. Sakai, Y. Taguchi, Th. Arima, Y. Tokura, *Nature Mater.* **8**, 558 (2009).

[6] S. Acharya, J. Mondal, S. Ghosh, S.K. Roy, P.K. Chakrabarti, *Mater. Lett.* **64**, 415 (2009).

[7] R.L. Wheit, *J. Appl. Phys.* **40**, 1061 (1969).

[8] G. Gorodetsky, L.M. Levinson, *Solid State Commun.* **7**, 67 (1969).

[9] J.-H. Lee, Y.K. Jeong, J.H. Park, M.-A. Oak, H.M. Jang, J.Y. Son, J.F. Scott, *Phys. Rev. Lett.* **107**, 117201 (2011).

[10] C.-Y. Kuo, Y. Drees, M.T. Fernández-Díaz, L. Zhao, L. Vasylechko, D. Sheptyakov, A.M.T. Bell, T.W. Pi, H.-J. Lin, M.-K. Wu, E. Pellegrin, S.M. Valvidares, Z.W. Li, P. Adler, A. Todorova, R. Küchler, A. Steppke, L.H. Tjeng, Z. Hu, A.C. Komarek, *Phys. Rev. Lett.* **113**, 217203 (2014).

[11] O. Pavlovska, L. Vasylechko, O. Buryy, *Nanoscale Res. Lett.* **11**, 107 (2016).

[12] Y. Tokunaga, S. Iguchi, T. Arima, Y. Tokura, *Phys. Rev. Lett.* **101**, 097205 (2008).

[13] Y. Du, Z.X. Cheng, X.L. Wang, S.X. Dou, *J. Appl. Phys.* **107**, 09D908 (2010).

[14] H. Wu, S. Cao, M. Liu, Y. Cao, B. Kang, J. Zhang, W. Ren, *Phys. Rev. B* **90**, 144415 (2014).

[15] W. Zhao, S. Cao, R. Huang, Y. Cao, K. Xu, B. Kang, J. Zhang, W. Ren, *Phys. Rev. B* **91**, 104425 (2015).

[16] O. Nikolov, I. Hail, K.W. Godfrey, *J. Phys. Condens. Matter* **7**, 4949 (1995).

[17] T. Suemoto, K. Nakamura, T. Kurihara, H. Watanabe, *Appl. Phys. Lett.* **107**, 042404 (2015).

[18] V. Derkachenco, V. Khokhlov, A. Kadomtseva, M. Lukina, *Solid State Commun.* **16**, 393 (1975).

[19] L. Akselrud, Yu. Grin, *J. Appl. Crystallogr.* **47**, 803 (2014).

[20] O. Pavlovska, L. Vasylechko, I. Lutsyuk, N. Koval, Ya. Zhydachevskii, A. Pieniążek, *Nanoscale Res. Lett.* **12**, 153 (2017).

[21] O. Pekinchak, L. Vasylechko, I. Lutsyuk, Ya. Vakhula, Yu. Prots, W. Carrillo-Cabrera, *Nanoscale Res. Lett.* **11**, 75 (2016).

[22] O. Pekinchak, L. Vasylechko, V. Berezovets, Yu. Prots, *Solid State Phenom.* **230**, 31 (2015).

[23] L. Vasylechko, A. Senyshyn, U. Bismayer, in: *Handbook on the Physics and Chemistry of Rare Earths*, Vol. 39, Eds. K.A. Gschneidner, Jr., J.-C.G. Bünzli, V.K. Pecharsky, North-Holland, Netherlands 2009, p. 113.

[24] M. Berkowski, J. Fink-Finowicki, P. Byszewski, R. Diduszko, E. Kowalska, R. Aleksijko, W. Piekarczyk, L. Vasylechko, D. Savytskij, K. Mazur, J. Sass, E. Kowalska, J. Kapusniak, *J. Cryst. Growth* **209**, 75 (2001).